

Multilayer bonding using a conformal adsorbate film (CAF) for the fabrication of 3D monolithic microfluidic devices in photopolymer

This article has been downloaded from IOPscience. Please scroll down to see the full text article.

2012 J. Micromech. Microeng. 22 085018

(<http://iopscience.iop.org/0960-1317/22/8/085018>)

View [the table of contents for this issue](#), or go to the [journal homepage](#) for more

Download details:

IP Address: 142.244.149.207

The article was downloaded on 06/08/2012 at 21:19

Please note that [terms and conditions apply](#).

Multilayer bonding using a conformal adsorbate film (CAF) for the fabrication of 3D monolithic microfluidic devices in photopolymer

L Gutierrez-Rivera^{1,5}, J Martinez-Quijada^{1,5}, R Johnstone², D Elliott¹,
C Backhouse³ and D Sameoto⁴

¹ Department of Electrical and Computer Engineering, University of Alberta, AB, Canada, T6G 2V4

² Teledyne DALSA, 18, boul. de l'Aéroport, Bromont (Québec) Canada J2L 1S7

³ Department of Electrical and Computer Engineering, University of Waterloo, 200 University Avenue West, Waterloo, Ontario N2V 1G3 Canada

⁴ Department of Mechanical Engineering, University of Alberta, AB, Canada, T6G 2G8

E-mail: sameoto@ualberta.ca

Received 25 March 2012, in final form 29 May 2012

Published 5 July 2012

Online at stacks.iop.org/JMM/22/085018

Abstract

Reliable microfabrication processes and materials compatible with complementary metal-oxide semiconductor (CMOS) technology are required by industry for the mass production of complex and highly miniaturized lab-on-a-chip systems. Photopolymers are commonly used in the semiconductor industry, and are suitable for the integration of multilayer structures onto CMOS substrates. This paper describes a novel photopolymer bonding process compatible with CMOS technology for the fabrication of three-dimensional monolithic microfluidic devices. The process consists of the formation of a conformal adsorbate film (CAF) approximately 15 nm thick on a patterned photopolymer layer (KMPPR), thereby increasing the number of open polymer chains at the bonding interface and acting as an ultra-thin adhesive layer. This thin adhesive layer is made of the same photopolymer as the microfluidic structures, but has a substantially lower crosslinking density so it will be able to make better bonds during a thermocompressive bonding step. This CAF treatment substantially improves the bonding yield between two patterned and previously crosslinked photopolymer layers because both optimum structure strength (to resist deformation during bonding) and bonding strength from epoxy crosslinking can be achieved. We demonstrate high bonding yields of up to 99% of the useful area of the substrate after three successive bonding steps. With this technique, up to six layers have been bonded in a single device. Unlike previously reported methods the quality of bonding is mostly decoupled from soft-bake parameters and crosslinking level of the previously patterned layers. Three different bonding processes were characterized to describe the bonding mechanism and the differences between the presented method and the partial-crosslinking bonding method. Capillary filling experiments were performed in microchannels of multilayer structures built with the CAF technique, without any observable leakage between layers.

(Some figures may appear in colour only in the online journal)

⁵ Equally contributing primary authors.

1. Introduction

Integration of complex 3D structures, such as microchannel networks [1], microvalves [2] and sensors [3], in the same device is becoming relevant in the development of lab-on-a-chip (LOC) systems, because several types of analyses are required to be performed on the same chip. These systems integrate one or more laboratory functions on a single chip of only millimeters to a few square centimeters in size. LOC devices are a subset of microelectromechanical system (MEMS) devices and are often referred to as micro-total analysis systems (μ TAS) as well. However, a true LOC system requires integration with complementary metal-oxide semiconductor (CMOS) technology to enable large-scale manufacture and cost reduction. The integration of different molecular biology operations in a LOC-CMOS device relies on the use of biocompatible materials and suitable microfabrication processes that allow for the formation of fluidic structures onto CMOS pre-processed wafers.

Several LOC systems are already being commercialized. The BioMarkTM systems use a micro-channel network for polymerase chain reaction (PCR) and genotyping applications [4]. The EOF Kit 9015 from Micronit microfluidics consists of a chip with borosilicate micro-channels and integrated electrodes for application in electrophoresis [5]. The i-STAT[®] cartridge technology from Abbot streamlines traditional lab operations by containing many of the components found in complex lab testing systems [6], but to have complete functionality and performance, the i-STAT[®] needs to be inserted into a separate device. These low cost, disposable devices have been commercially successful and yet all these products still require external electrical, mechanical and optical interfaces, since effective integration of many necessary system components has yet to be attained. We believe that the development of CMOS-compatible polymer multilayer architectures is crucial to achieving maximum miniaturization and integration of the fundamental molecular biology operations in a single chip.

The choice of material for the fabrication of microfluidic structures is crucial for integration onto CMOS microelectronics. The introduction of polymers in MEMS has proven to be one of the recent key developments of these fields [7]. The availability of a wide range of materials with suitable properties has enabled many new applications in microfluidics and other research areas where material properties such as wettability, transparency, dielectric strength, thermal conductivity, elasticity and biocompatibility need to be carefully controlled.

Photo-patternable polymers, or photoresists, have been traditionally used to transfer a design to a thin film using photolithography, but more recently have also been used as structural materials in microfluidics. *SU-8*, a negative tone photoresist patented by IBM in 1989, is perhaps the best example of a photopolymer used to construct an ample variety of structures. Its good chemical compatibility and biocompatibility [8] makes *SU-8* suitable as a structural material for the fabrication of microfluidic devices [9–11].

The integration of thin film heaters and sensors into photopolymer-based LOC systems demands strong adhesion

of the photopolymer to metals. The adhesion, as well as the structural integrity of the photopolymer, must be unaffected by moisture since aqueous solutions are to be handled. Recently, KMPR (MicroChem Corp) has emerged as a new photopolymer alternative with photolithography characteristics similar to those of *SU-8* [12]. But unlike *SU-8*, KMPR is less susceptible to cracking during lithography [13] and has excellent adhesion to metals [13–15]. If KMPR and *SU-8* are deposited on Al/Cu, and then left in a moist environment, *SU-8* loses adhesion quickly, while KMPR maintains a strong adhesion, even for several days [14]. From this perspective, KMPR appears to be a better choice for the fabrication of CMOS compatible multilayer LOC systems.

Microchannels have been fabricated in photopolymers such as KMPR [16] and *SU-8* [17–20] for different applications. In one of the simplest techniques, microchannels are encapsulated by joining two wafers using adhesive bonding [16, 21–23]. The floor and walls of the channels are fabricated on one wafer and the roof is fabricated on a second wafer. A thin film of the same photopolymer is spun on the unpatterned roof layer to work as an adhesive, or else the roof layer itself may be used as an adhesive. Keeping the adhesive layer in liquid form produces bubbles and capillary filling of channels when the wafers are contacted. These effects can be reduced with a full soft-bake [16] or a partial soft-bake [22] to render the film solid or semi-liquid. However, the wafers need to be heated and pressed for the adhesive to comply with the mating surface and polymerize. Due to this applied pressure, the adhesive film is able to flow, potentially clogging the channels and other features. To cope with this, alternate channels/cavities can be cut around the device channels to accommodate the excess adhesive [22], or the adhesive layer can be as thin as 3 μ m to reduce the amount of material flowing into the channels [23]. In both cases, the channels are still susceptible of filling and this imposes a limit on the smallest channels that can be made. Furthermore, conventional adhesive layers can only be spun on unpatterned surfaces, limiting the use of adhesive bonding to the fabrication of simple structures requiring a single bonding step. However, a complete and highly functional LOC system requires more than two layers and two or more bonding steps to incorporate microvalves, electrodes, heaters, sensors, channels, chambers and inter-layer fluidic and pneumatic vias. This is only possible in a multilayer architecture and this requires multiple bonding steps of pre-patterned films.

Previous reports have shown the feasibility of bonding two or more layers of photopolymers using a carrier-release technique to construct complex microfluidic structures in photopolymers [21, 22]. The technique consists of coating a carrier wafer with a low-adhesion material prior to the deposition of the photopolymer. The structural photopolymer is transferred from the carrier wafer to the device wafer after bonding due to the low adhesion between the release layer and the transferred material. The carrier wafer can be released as long as the interfacial photopolymer adhesion is larger than the adhesion of the photopolymer to the release layer. Other methods employ a sacrificial layer to hold the photopolymer on the carrier wafer, and after bonding the

carrier is released by etching the sacrificial layer [21–22]. This method, however, requires additional process steps and long times for the etchant to flow through the thin clearance under the photopolymer layer. Most importantly, the etchant and the dissolved material can contaminate the chip by invading the microchannels and cavities, rendering the device unusable for biological applications.

Within the category of sacrificial materials, polypropylene carbonate (PPC) and poly-ethylene carbonate (PEC) have been used as a sacrificial layer for the fabrication of *SU-8* microchannels [24]. These materials were heat-depolymerized at high temperature after *SU-8* was patterned on top to form microchannels. This dramatically speeds up the removal times for the sacrificial layer in comparison to wet etched sacrificial materials. Trichlorosilane and dimethyldichlorosilane may also be used as sacrificial layers for the fabrication of microchannels using heat-depolymerization [25]. All these materials need elevated temperatures (150–250 °C) to evaporate, which may produce high stresses in the photopolymer film that could potentially delaminate the structure. Additionally, depolymerization may not be complete, and so the sacrificial material may leave residues behind, causing similar problems with final device performance as other sacrificial materials.

Another technique to produce microchannels without a sacrificial layer is to build each layer separately then bond them together using techniques like lamination or thermo-compressive bonding. To do so requires that each transferred layer be patterned on a material with relatively low adhesion to the structural material, so as to ensure that it will transfer without damage. Typically, a material with low chemical affinity to the structural photoresist or low surface energy is used as a release layer. Within the category of release layers, polyester (PET) in the form of a foil is used to coat the carrier wafer by lamination [26, 27], and then peeled off both the substrate and the transferred structure to form microchannels. A Teflon film is another low-adhesion alternative used to coat the carrier wafer when producing *SU-8* microfluidic devices for use in dermal patches [28]. Finally, Kapton™ is a polyimide used also on the carrier wafer [29] for the fabrication of *SU-8* multilayer devices. According to the authors, *SU-8* may remain stuck on the Kapton™ film during the release, producing damage to the structure. The severity of the damage varies with the type of the structure patterned in the photopolymer [29].

Lamination is often used to encapsulate photopolymer microchannels that transfers uncrosslinked [26] or partially crosslinked [27] layers, and then crosslinks them together by applying heat and pressure to produce a permanent attachment. In, the first instance, a roof photopolymer layer was spun and dried on a transparent and flexible foil, and then bonded onto a pre-patterned and crosslinked layer [26]. The flexibility of the carrier foil helped to produce good contact between the bonding layers only with the pressure of a manual roller. The transparency of the foil also allowed easy alignment and backside UV lithography of the roof layer, which triggered crosslinking of the roof layer. After bonding, exposure and crosslinking, the carrier foil was released owing to its poor

adhesion to the photopolymer. In a similar process, the photopolymer layer on the carrier foil was first patterned, partially crosslinked and then bonded onto a layer that had been previously patterned and fully crosslinked [27]. These techniques require careful control of baking time and temperature to achieve acceptable bonding while preventing deformation of the structures from pressure or filling the channels with the photopolymer material. These difficulties arise because the photopolymer is soft when it has been prebaked but not crosslinked (or only partially crosslinked) and thus can easily deform or flow with the application of heat and pressure. Due to the softness of these films, the bonding pressure cannot be increased above a certain limit to enhance contact. In the case of lamination with partially crosslinked layers, the photopolymer can be hardened further by increasing post-exposure bake (PEB) time/temperature, but as the crosslinking level of the film increases the probability of strong bonding and hence the bonding yield decrease.

With the partial crosslinking lamination technique, multilayer bonding yields of ~80%, in terms of bonded area, have been obtained after three bonding steps using Kapton on the carrier wafer [29]. In terms of number of finalized bonded chips, multilayer bonding yields of 80% have also been reported using PET as a carrier foil [27]. The bonding yield is known to decrease with an increase in the number of bonding steps. In [29], for example, the bonded area diminished from 95% in the first bonding step to 80% in the third step. This lowered yield can be attributed to the increased surface unevenness after successive thermo-compressive bonding steps [29]. Unevenness is created by the deformation under high pressures of the partially crosslinked layers, which are mechanically less resistant than highly crosslinked layers. The topography then reduces contact in future bonding steps, and without good contact during bonding, voids and other defects may occur. The quality of bonding therefore depends largely on both the level of partial crosslinking of the photopolymer established before bonding and the planarity of the layers before and after bonding [29]. In this work, we have developed a novel bonding process for the fabrication of complex multilayer structures in the KMPR photopolymer. These structures are demanded by highly integrated LOC systems and our process is compatible with the CMOS technology. Unlike previously reported methods [27, 29], the process presented here supports the fabrication of high-quality monolithic multi-layer structures with at least six layers individually patterned and bonded one by one, with 90–100% bonded area after five bonding steps. This new approach does not require strict control of the soft-bake parameters and is independent of the crosslinking level of the photopolymer layers being bonded.

The process allows fabrication of microreactors, inter-layer vias and microchannels for fluidic and pneumatic interconnects; this could potentially permit fabrication of microvalves and metallic thin film components such as heaters, sensors and electrodes embedded between layers. This process has been developed to enable cost-effective manufacture of fully integrated single-chip LOC systems capable of carrying out complete genetic analyses for the

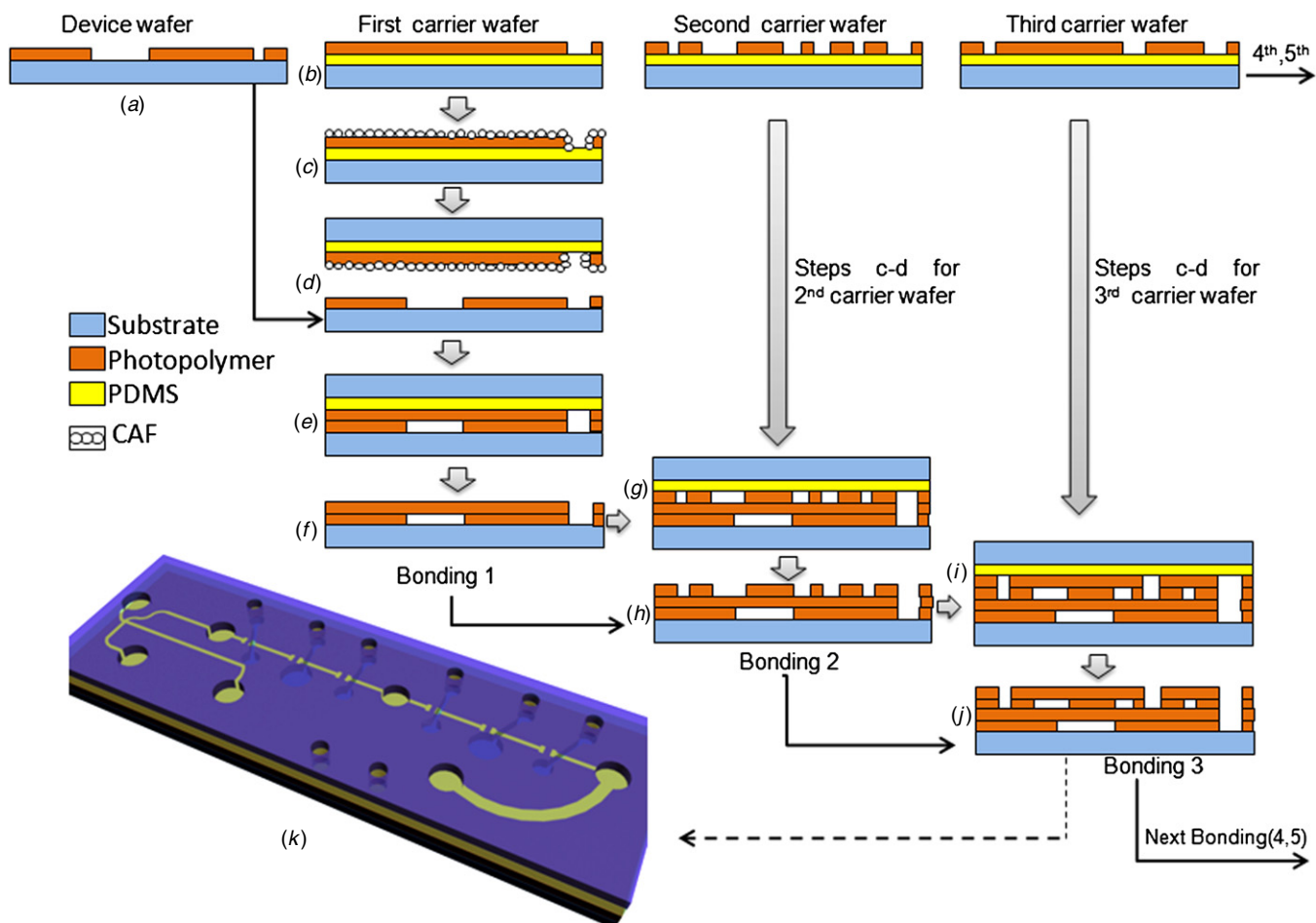


Figure 1. Schematic diagram of the fabrication process. (a) Photolithography of the first layer on the device wafer. (b) Photolithography of layer 2 on KMPR on a PDMS film, first carrier wafer. (c) Conformal coating of the patterned KMPR with the CAF. (d) Alignment and assembly. (e) Bonding by thermo-compression. (f) Carrier wafer release. (g) Bonding of layer 3 on the device wafer. (h) Second carrier wafer release. (i) Bonding of layer 4 on the device wafer. (j) Third carrier wafer release. (k) Three-dimensional perspective of the completed four-layer chip, showing fluidic/pneumatics channels.

detection of infectious diseases, cancer and deficiencies (e.g. adverse drug reactions). To reach their expected potential, these systems must incorporate the most essential molecular biology operations such as sample preparation (SP), genetic amplification through the PCR and analysis/detection through capillary electrophoresis (CE). We believe that the multilayer photopolymer architecture is the most suitable means to group the variety of electrical and fluidic components required for each of these operations onto a compact device, and a reliable high-quality wafer-level bonding process is key in this architecture.

2. Fabrication

Figure 1 shows the process for the fabrication of a multilayer structure in the photopolymer. The process starts with the cleaning of the glass substrates. Onto the first substrate (device wafer, figure 1(a)), we build the bottom layer by photolithography, and the layer is crosslinked with a PEB at $\sim 100^\circ\text{C}$ for 5 min. Simultaneously, on a second substrate (carrier wafer), a cured polydimethylsiloxane (PDMS) film is formed, (figure 1(b)). The PDMS used in this work was

Sylgard[®] 184 mixed at a ratio of 10:1 base to catalyst. On the PDMS film, a second KMPR layer is patterned up to and including development, and then crosslinked (figure 1(b)) using standard PEB temperatures. A surface treatment is performed to deposit a conformal adsorbate film (CAF) on the top surface of the carrier wafer (figure 1(c)), described in detail later, and the wafers are subject to a thermal treatment to harden the photopolymer to avoid deformation during thermo-compression. The device wafer and the carrier wafer are aligned and brought into contact (figure 1(d)). Thermo-compression is carried out to press the layers against each other and crosslink the CAF at the bonding interface, joining them permanently (figure 1(e)). After bonding, the carrier wafer can be released due to the poor adhesion between PDMS and KMPR (figure 1(e)). After release, two layers of the final device are completed (figure 1(f)). The next layers are added by repeated bonding and release steps (figures 1(g)–(j)). Using this process, structures of up to six layers were constructed with five bonding steps. Figure 1(k) shows a 3D perspective of the finished four-layer microfluidic structure.

2.1. Wafer preparation

We used borofloat glass substrates of 10 cm × 10 cm × 1.1 mm. To improve the adhesion with the photopolymer, the substrates were cleaned in a piranha solution (sulfuric acid: hydrogen peroxide, 3:1). The substrates were then dehydrated in an oven at 150 °C for 15 min. Two kinds of wafers were prepared: a device wafer and multiple carrier wafers. On the device wafer the layers of the structure are added one by one by successive bonding and release steps. On the carrier wafers, each layer to be added is photo-patterned individually.

2.2. Lithography process

2.2.1. Device wafer. The process starts with the deposition and patterning of the first KMPR film on the glass substrate. This film was spin-coated to a thickness of ~56 μm, before being exposed to 1000 mJ cm⁻² of UV light (365 nm) through a mask. The exposed film was post-exposure baked at 100 °C on a hotplate and developed with a MF319 solution, rinsed in deionized water, and dried with nitrogen gas.

2.2.2. Carrier wafers. PDMS that had been previously mixed and degassed under vacuum is spin-coated on a glass substrate at 3000 RPM and cured for 3 h at 80 °C, resulting in a 5 μm thick PDMS film. PDMS is used because of its low stiffness and low adhesion to the photopolymer. The adhesion of prebaked KMPR to PDMS is high enough to carry out lithography on it, but low enough to permit release of the carrier wafer after bonding [30]. Due to the low surface energy of PDMS, dewetting of the KMPR in solvent may occur during pre-bake causing voids and non-uniformities on the film, usually beginning from the edge of the wafer, and occasionally resulting in a total collapse of the photopolymer film under its own surface tension. To prevent this effect, a square piece of glass is placed and centered on the cured PDMS film, covering most of its area, and 20 nm of Au is sputtered atop. This creates a perimeter of higher adhesion material which serves as an anchor for the photopolymer at the edges of the PDMS film. This anchor prevents the majority of dewetting problems during pre-bake.

Thereafter, KMPR is spin-coated on the PDMS film to a thickness of 56 μm. The photopolymer is normally stored in a fridge and must be taken out and left to warm at room temperature for at least 2 h before use in order to obtain highly uniform films. After spinning, the wafer is soft-baked by increasing the temperature in three steps: 20 min @ 60 °C, 20 min @ 80 °C, and 20 min @ 100 °C (each step is performed on a different hotplate). This incremental soft-bake minimizes dewetting of KMPR while it still contains solvent.

The wafer was then exposed (1000 mJ cm⁻², 365 nm) with the mask for layer 2 of the microfluidic device, followed by a PEB at 100 °C for 3 min and developed in MF319 for 9 min. Verification that the channels are totally open and clean is done through visual inspection. Finally, the wafer is rinsed with DI water and dried with nitrogen gas.

2.3. Conformal adsorbate film (CAF)

After patterning the KMPR layer on the carrier wafer, it is given a surface treatment to form a barely polymerized molecular-scale KMPR CAF of ~15 nm thickness. First, a KMPR-1005/cyclopentanone solution is prepared in concentration 1:4 with strong agitation to obtain a homogeneous mix. Next, the carrier wafer with the patterned KMPR layer is immersed horizontally in this solution for 2 min. Evaporation of solvent at room temperature is slow and so the volume of solution and the KMPR concentration remain almost constant over 2 min of immersion. The wafer is not agitated while immersed in the solution. The solution invades channels and cavities completely, resulting in a conformal coating of all surfaces.

After 2 min, the wafer is taken horizontally out of the container and the excess solution is dripped off with a slight tilt. The wafer is allowed to dry at room temperature for 20 min on a flat surface, which evaporates part of the solvent (cyclopentanone). At the end of this period, the surface of the patterned layer is sticky to touch because the KMPR deposited in solution has not been soft-baked. The wafer is then soft-baked for 1 min at 65 °C. At the end of this step, channels and other features in the patterned KMPR layer are clogged with a surplus non-uniform KMPR coating visible to the naked eye.

The wafer is then blanket-exposed to 400 mJ cm⁻² of 365 nm light to produce the catalyst that will trigger polymerization during bonding. After exposure, the surplus KMPR is removed with MF319 developer for ~2 min with slow agitation without completing a PEB first. This allows thicker KMPR in the channels to be removed by the developer while leaving a very thin layer of barely crosslinked KMPR on all surfaces. The wafer is taken out from the developer, immediately placed in a container with DI water and agitated slowly for ~2 min until the channels and other features look totally clean. Once the excess KMPR is removed, the wafer is dried with N₂ gas and left at room temperature for 20 min for any liquids remaining in the CAF to evaporate. The wafer is then placed on a hotplate at 60 °C for 30 min and thereafter at 80 °C for 40 min to harden the patterned KMPR structure and the CAF in preparation for bonding. During this process the ambient temperature was 20 °C and relative humidity was 45%.

2.4. Bonding

The bonding process is performed using an embosser (Jenoptik HEX02). Figure 2 shows the setup for bonding. The entire device area (8 × 8 cm²) is pressed between two 1/16" thick square polycarbonate pieces. The device wafer and carrier wafer are aligned, brought into contact and positioned in the embosser, which presses them with a force of 25 kN. After reaching the target pressure, the embosser heats up the wafers to 100 °C (~5 °C min⁻¹) to trigger crosslinking of the CAF with the surfaces of the patterned layers at the bonding interface. The contact is maintained for 15 min at 100 °C before the substrates are cooled and the pressure removed. After bonding, the carrier wafer is released carefully by slowly peeling the KMPR off of the PDMS perimeter with a razor blade, leaving the two KMPR layers bonded irreversibly on

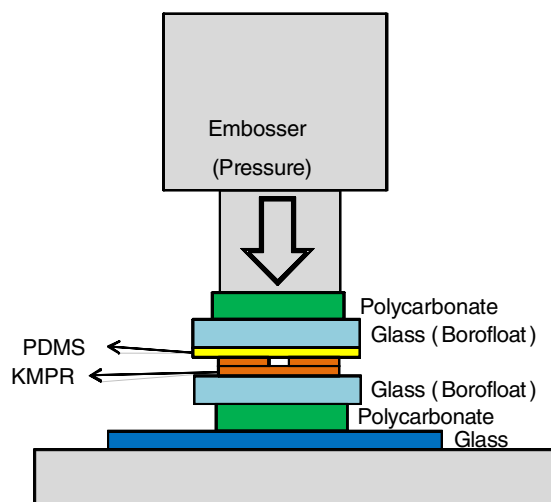


Figure 2. Thermo-compressive bonding setup.

the device wafer. This process is repeated by patterning the subsequent layers on different carrier wafers and bonding them on the stack one layer at a time until the structure is completed on the device wafer. With this technique, up to six layers were joined with five bonding steps.

3. Results and discussion

3.1. Lithography process

Performing lithography of KMPR on PDMS must be done carefully to obtain clean features and establish a level of polymerization that provides the necessary mechanical strength to survive the thermo-compressive bonding process. Owing to the high penetration of UV light through KMPR, doses in the range of 900–1500 mJ cm⁻² can yield well-patterned channels, but lower doses can result in structures with low levels of polymerization resulting in deformations when heat and pressure are applied during bonding.

When using the CAF bonding technique, the patterned KMPR layer is post-exposure baked at 100 °C for 3 min to crosslink the layer. When using the partial crosslinking bonding method, the PEB temperature (90 °C) should be lower than the bonding temperature (100 °C) in order to leave a large number of free monomers in the film, sufficient to achieve bonding. The PEB temperature of 90 °C was chosen because it is the lowest temperature that we found to get patterned structures with good resolution after development. The crosslinking of the layer is then completed inside of the embosser.

3.2. Film uniformity

High uniformity of the photopolymer film (flatness) makes it possible to produce intimate contact between KMPR layers during thermo-compressive bonding. Before spin-coating, the photopolymer should have a uniform viscosity at room temperature and a reliable technique for the casting of the photopolymer should be used [31].

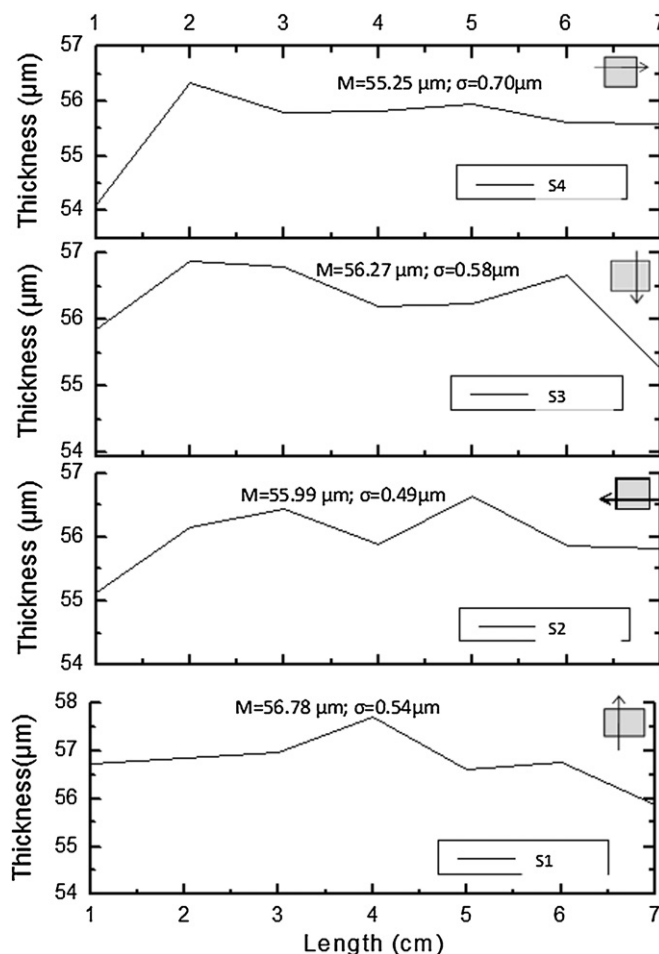


Figure 3. Surface profile of a patterned and crosslinked KMPR film along four different paths in the same sample, obtained by profilometry. The film was fabricated on a carrier wafer onto a PDMS film. M is the mean thickness; σ is the standard deviation.

Abrupt temperature changes during soft-baking produces dewetting of epoxy-based photopolymers on PDMS [30, 32]. This effect can be reduced by ramping the temperature after spin coating [30]. For a KMPR film 56 µm thick, we performed the soft-bake in periods of 20 min at 60, 80 and 100 °C to evaporate the solvent slowly and minimize dewetting.

To measure the uniformity of the film, the patterned KMPR layer was scanned by profilometry over an area of 7 × 7 cm². Thickness measurements at the edge of channels and wells were used to make a profile of the surface. The KMPR film had an average thickness of ~56 µm and maximum standard deviation of 0.7 µm. Figure 3 shows the profile of the polymerized KMPR film along four different paths on the film.

3.3. Conformal adsorbate film (CAF)

The surface treatment described in section 2.3 resulted in the formation of a conformal film approximately 15 nm thick formed by the adsorption of monomers in the solution onto the surface of the patterned photopolymer. The thickness was measured using an optical profilometer to avoid contact with the surface and so ensure the integrity of the CAF. Figure 4

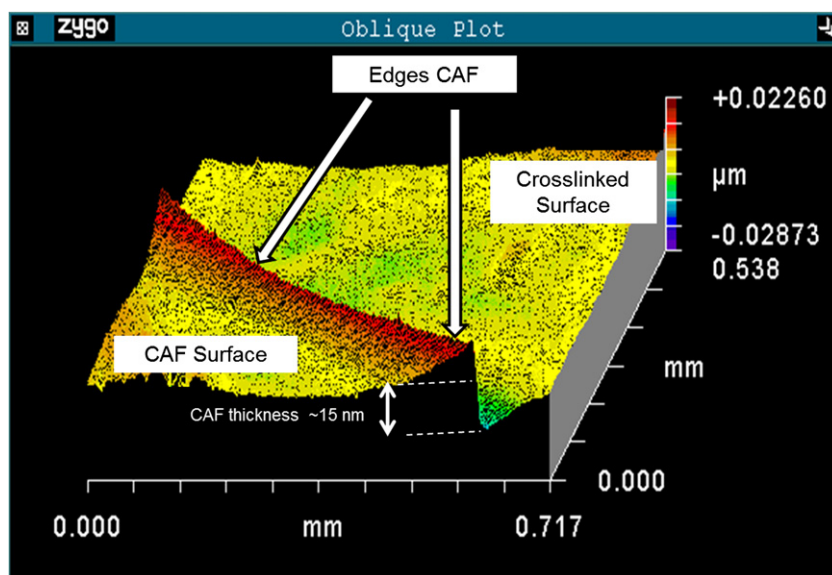
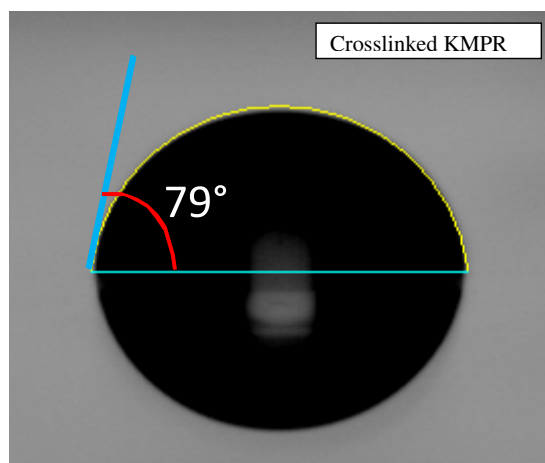


Figure 4. Optical profilometer image of the conformal adsorbate film (CAF), formed on the surface of a crosslinked 56 μm KMPR layer. To create a step in the CAF, a drop of PDMS was placed on the KMPR layer and allowed to extend over the surface; the drop was then cured and the wafer was coated with the CAF; finally, the drop was lifted off to cut a step in the CAF. When the KMPR/cyclopentanone solution is applied, surface tension raises the profile of the CAF at the boundary of the PDMS drop, which creates a lifted edge when the drop is removed. Because of this, the thickness of the CAF is measured far from the edge, where the CAF exhibits its best uniformity.

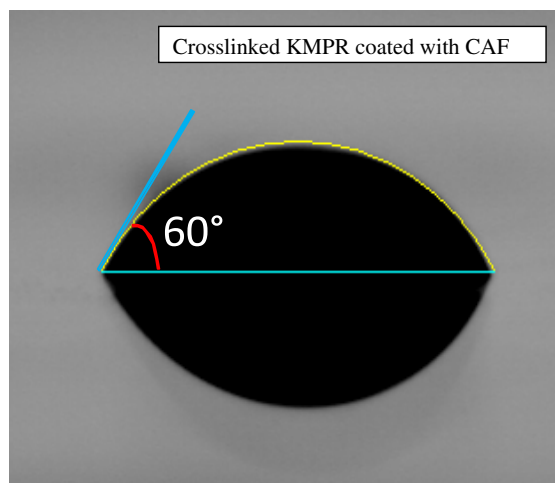
shows the profile of a step in this conformal film on the surface of a fully crosslinked KMPR layer of 56 μm thickness. The step in the conformal film was created by placing cured PDMS drops on the crosslinked KMPR layer before forming the conformal film and lifting-off the cured PDMS.

To obtain a metric of the polymerization level of the CAF, we first measured the contact angle of DI water on reference soft-baked (non-crosslinked) and crosslinked KMPR layers. Secondly, we measured the contact angle on the CAF and compared it to the reference. A surface with monomers whose bonds are free will show higher energy than the surface in which most of the bonds have been passivated by the linking to other bonds. Since higher surface energies manifest in lower contact angles, we expected that the CAF would show low contact angles, approaching those of soft-baked KMPR, and hence would have similar bonding potential. Figure 5 illustrates the variation of the contact angle before (79°) and after (60°) of the surface treatment. When KMPR is crosslinked, the contact angle increases and therefore the hydrophobicity of the surface can provide a rough proxy for the degree of crosslinking of the surface. The contact angles showed standard deviation of $\pm 3^\circ$. Notably, the contact angle on the conformal film is very similar to that of regular soft-baked KMPR film ($\sim 60^\circ$). When, the conformal film was crosslinked, the contact angle increased to $\sim 69^\circ$, lower than the contact angle on a regular crosslinked KMPR film.

The thickness of the CAF will depend on the concentration of monomers in the KMPR-1005/cyclopentanone solution. For a concentration of 1:7, respectively, the thickness is ~ 7 nm and for 1:3 the thickness is ~ 25 nm. A concentration of 1:4 is the most appropriate and results in CAF thickness of ~ 15 nm. Larger amounts of solvent lead to detachment of the patterned KMPR from the PDMS on the carrier wafer, which hinders bonding. Conversely, higher concentrations of KMPR may produce a non-uniform coating with clumps.

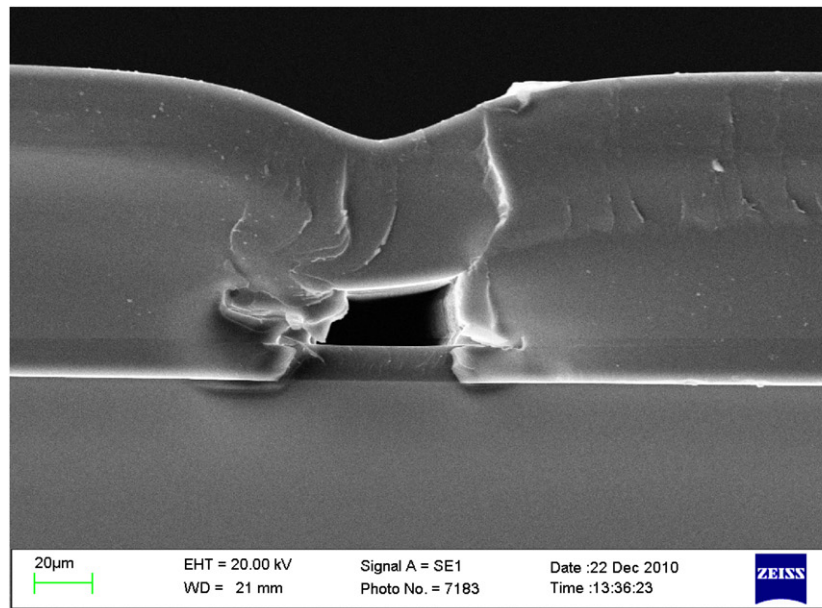


(a)

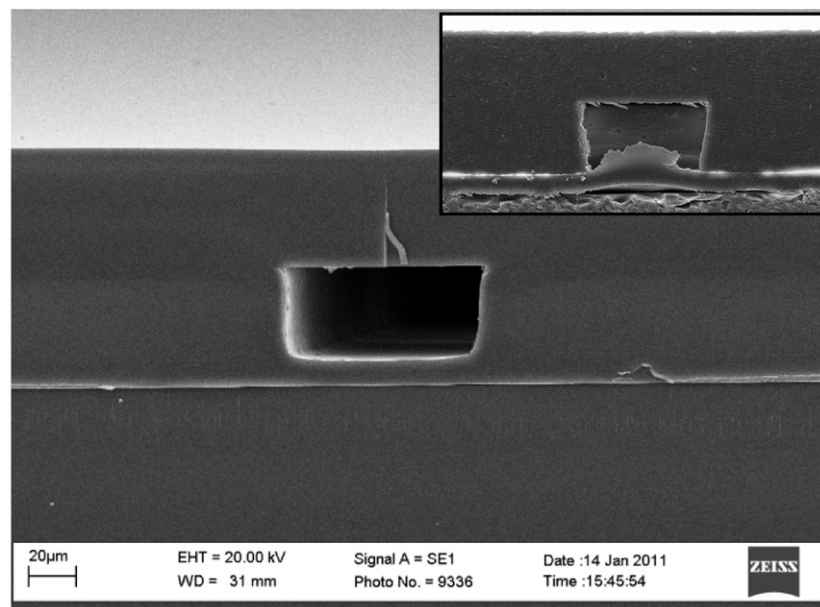


(b)

Figure 5. Contact angle on the surface of a crosslinked KMPR film, (a) without CAF and (b) coated with the CAF.



(a)



(b)

Figure 6. SEM cross-sectional image of microchannels in KMPR, (a) without post-development bake after CAF coating. (b) With post-development-bake PDB after CAF coating. These treatments harden the layer to be bonded, which reduces deformation substantially; cracks on the vertical face of the roof layer are caused when the sample is cut by freezing with liquid nitrogen. Inset: another example (cross section) of a microchannel created with a PDB-hardened roof; dicing the sample with a diamond saw prevents facial cracks on the roof layer, but the floor layer delaminates and debris clogs the channel entrance.

The creation of the CAF allocates functional groups of the photopolymer along the surface of the patterned KMPR. Also, since the wafer is exposed during the surface treatment, the amount of the catalyst that promotes crosslinking increases in both the patterned KMPR film and the CAF. When a substantial amount of open-chain KMPR monomers and catalyst is distributed uniformly, there will be enough free monomers during thermo-compression to enable effective linkage of the mating layers during bonding.

3.4. Deformation of structures during bonding

Deformation of the patterned structures will likely occur during bonding (figure 6(a)) because the solvent (cyclopentanone) permeated into the KMPR structure during the surface treatment described in section 3.3 to form the CAF. This is why, in addition to properly soft-baking and crosslinking the photopolymer as described in section 3.1, it is essential to apply an additional thermal treatment before bonding. This treatment consists of a post-development

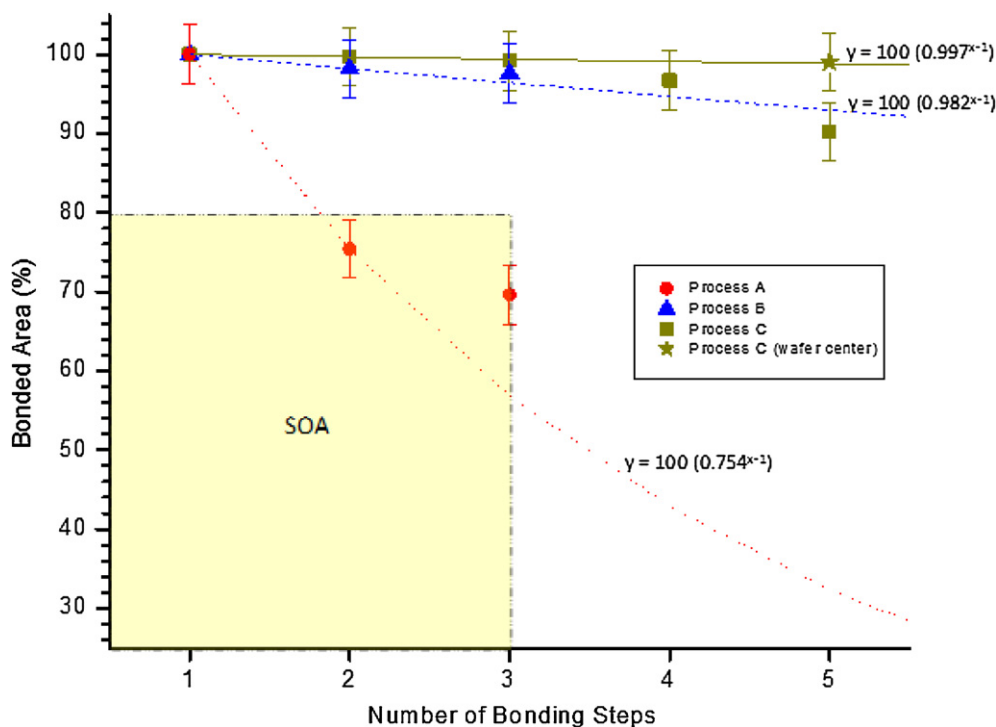


Figure 7. Graph of the bonding yield versus number of bonding steps. SOA is the state of art before this work. A is the non-optimized partial crosslinking method; B is the improved partial crosslinking method; C is the CAF method.

bake that provides the structure with enough mechanical resistance to withstand thermo-compression. Heating the carrier wafer to ~ 60 °C for 10 min and then to ~ 80 °C for 40 min makes the structures more rigid and minimizes deformation (figure 6(b)). If the solvent is evaporated too quickly, the KMPR film detaches from PDMS; low temperatures in a two-step ramp avoid this effect.

3.5. Multilayer bonding characterization

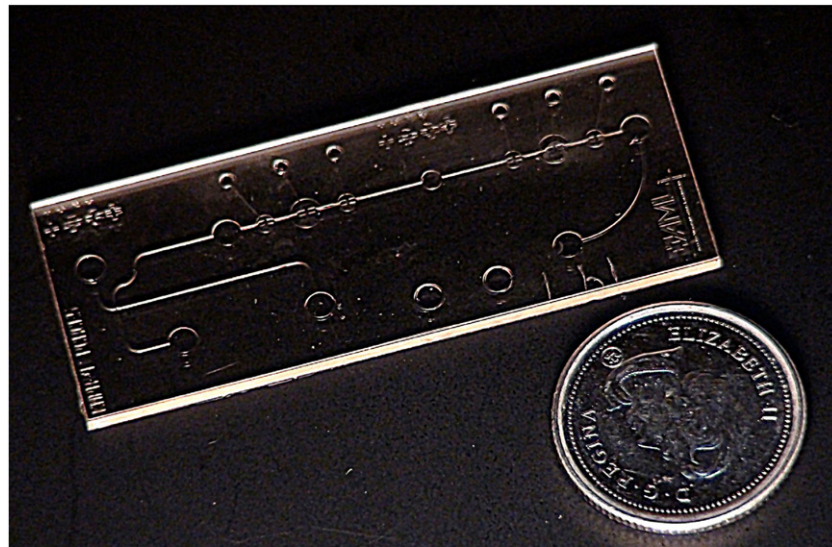
The quality of bonding was assessed in terms of the percentage of bonded area, measured after each bonding step over the entire bonded layer (all layers have a total footprint of 8×8 cm²). For this purpose, a transparent plastic sheet with a printed square grid of 1 mm spacing was placed underneath the wafer and the unbonded areas were measured by counting the number of squares. Unbonded or defective regions were also measured from wafer-wide photographs, always taken at the same angle and distance.

Figure 7 shows the percentage of the bonded area for three different bonding processes performed at the same bonding temperature (100 °C). In process A (partial crosslinking bonding method), each layer on the carrier wafer was post-exposure baked at 100 °C for 3 min. After three bonding steps (four-layer structure), a bonded area of 70% was observed. To improve bonding yield, the post-bake temperature was reduced progressively until obtaining the highest yield for the three bonding steps while maintaining sufficient stiffness of the structure to withstand the bonding pressure without being deformed. The yield increased to 80% and 96% when reducing the PEB temperatures to 95 and 90 °C, respectively, for the three bonding steps. The level of partial crosslinking was also

controlled by time. Using a PEB temperature of 100 °C, no significant change in the yield was observed when PEB time was varied from 3 to 2 min. With a 1 min PEB time, part of the structure dissolved during development.

In process B (improved partial crosslinking bonding method), multilayer bonding was performed using a PEB temperature of 90 °C. As a result, the bonded area after three bonding steps grew to 96%.

In process C (CAF bonding method), each layer to be bonded was crosslinked with a 100 °C post-exposure bake during 3 min, and thereafter the surface treatment was performed to create the CAF on the surface. After three bonding steps, a bonded area of 99% was measured. Fourth and fifth bonding steps (five and six-layer structures) were also performed with the CAF technique and the bonded areas were 97% and 90%, respectively. In the fifth bonding step, narrow unbonded bands at the edges of the wafer near the corners appeared, causing an abrupt drop in the percentage of total bonded area inconsistent with the trend line. We attribute the appearance of these unbonded regions to the accumulated loss of flatness at the corners and edges over repeated thermo-compression cycles, which reduces the quality of bonding in subsequent layers. This reduced planarity at the corners builds up with each layer, and at the fifth bonding step the loss of planarity starts to extend along the edges, which produces the abrupt decay of total bonded area to 90%. In contrast, at the center of the wafer the structure is loaded more uniformly and has fewer perimeter related thickness defects, thus good contact and planarity are maintained. This results in a bonded area that approaches 100% in a 4.5×4.5 cm² area at the center portion of the wafer after five bonding steps. In this center region, we have excluded poorly bonded areas



(a)



(b)

Figure 8. (a) Four-layer chip for complete genetic analysis that integrates PCR, CE and SP sections, 45×17.5 mm. (b) Four-layer chips for CE analysis and detection, located at the center of the wafer. The logo area, on the top-right corner of each chip, as well as the alignment marks on the opposite corner, were excluded when measuring the bonding yield in this center portion of the wafer.

of 3×7 mm² from each of the six 1.5×2.25 cm² area chips. These defects occur within the region our logo is patterned. The characters of the logo are formed by a set of cavities cut into the first layer in very close proximity to each other. Therefore, the layers bonded on top find significantly lower reaction force, and the small features between cavities are distorted under the high pressures used which results in poor bonding. Because of this, we recommend to allow at least a $500 \mu\text{m}$ separation between contiguous cavities for effective bonding. In the rest of the chip area outside the logo, the bonding yield is nearly 100% across five bonding steps.

The PEB temperature, time temperature and bonded area for the processes A, B and C are listed in table 1.

The carrier wafer and device wafer were aligned manually with an optical microscope, using alignment marks patterned on every layer. The largest alignment error between two adjacent layers was found to be $\sim 20 \mu\text{m}$. This error could be reduced substantially by holding the carrier wafer on a mask aligner, with a custom-made adapter, and then positioning the carrier wafer underneath via the multi-axis micro-positioning stage of the equipment.

Table 1. Process parameters of the three bonding techniques for the KMPR layer on the carrier wafer. The same parameters were used in all bonding steps of each technique. In all cases, the bonded area in the first step was 100%. In the process C, the KMPR was crosslinked before applying the CAF. Wafer area $8 \times 8 \text{ cm}^2$. Measurement area on wafer center $4.5 \times 4.5 \text{ cm}^2$.

Process	PEB temperature ($^{\circ}\text{C}$)	PEB time (min)	Bonded area (%)	Number of bonding steps achieved
A (partial crosslinking)	100	3	70	3
B (optimized partial crosslinking)	90	3	96	3
C (CAF coating)	100	3	99	3
	100	3	99 wafer center 90 whole wafer	5

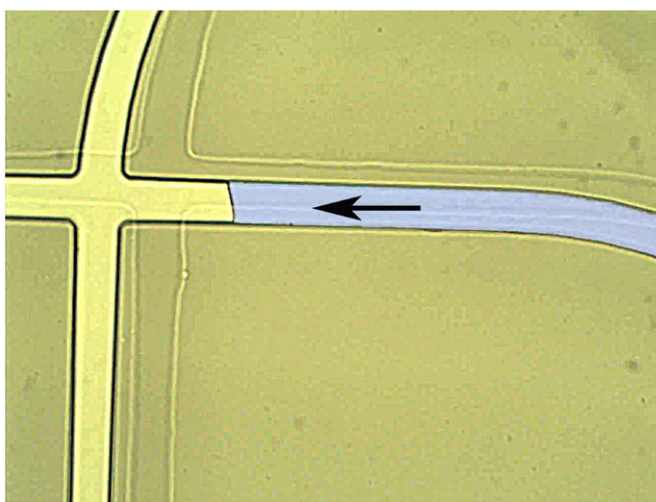


Figure 9. Capillary filling of DI water in KMPR microchannels. The arrow indicates the position of the advancing meniscus.

Figure 8(a) shows a complete four-layer chip with a PCR chamber, microvalves and fluidic/pneumatic microchannels and ports. Figure 8(b) shows four-layer chips for CE analysis and detection located at the center of the wafer. The logo area (top-right corner of each chip) and the alignment marks (opposite corner) were excluded when measuring the bonding yield in the center portion of the wafer.

3.6. Leakage and bonding strength tests

We carried out capillary filling experiments in microchannels of three- and four-layer chips built with the CAF technique. The channels self-filled at a rate of $74 \mu\text{m s}^{-1}$ with DI water, showing no discernible leaks between layers. The experiments were repeated after passing isopropanol through the channels and allowing it to evaporate. This treatment increased filling velocity of DI water to $110 \mu\text{m s}^{-1}$. Again, no leakage of isopropanol or water was observed, indicating a tight seal of the layer-layer interfaces. Figure 9 shows a sequence of snapshots of the capillary filling in microchannels. Bonding strength was tested by applying pressurized air into $100 \times 50 \mu\text{m}$ channels closed at one end, in chips of four $56 \mu\text{m}$ thick layers, finding that the structure starts to delaminate at 65 psi ($\sim 448 \text{ KPa}$). For *SU-8* micro-channels, liquid pressure up to 600 KPa before leakage has been reported [29].

Since no leakage was observed during capillary filling and the maximum pressures used to actuate microvalves in the chip is 30 psi ($\sim 206 \text{ KPa}$), we believe that the CAF bonding technique is well suited to build multilayer structures for microfluidic applications.

4. Conclusions

We presented a new approach for the fabrication of three-dimensional monolithic multilayer structures by joining patterned and crosslinked photopolymer (KMPR) layers using a novel CAF bonding technique. This technique enables cost-effective fabrication of LOC systems with complex networks of fluidic/pneumatic microchannels, inter-layer vias, microvalves and other microfluidic components. Being a low-temperature high bonding yield process, the CAF technique allows integration of microfluidics and CMOS microelectronics in a single chip.

To build a multilayer structure, individual KMPR layers are fabricated on a carrier wafer and subsequently bonded onto each other before releasing the carrier wafer. The CAF bonding technique consists in the formation of a thin conformal film of $\sim 15 \text{ nm}$ thickness on the surface of one of the bonding KMPR layers. This film substantially increases the availability of open polymer chains at the bonding interface, enhancing the probability of linkage between mating layers. The technique has shown a maximum bonding yield of 99% over the total area of the patterned layers after three bonding steps (four-layer structure), and 90% after five bonding steps (six-layer structure). The yield decays due to delamination and lower pressure at the corners of the wafer, while the central, defect-free, portion of the wafer has a near 100% yield after five bonding steps.

Unlike previously reported photopolymer bonding methods that rely on partial crosslinking of one of the bonding layers, the CAF technique allows a high-quality bonding of pre-patterned and crosslinked KMPR layers. Therefore it is not necessary to keep a strict control of soft-bake and PEB parameters of the layers to be bonded.

Besides the CAF technique, we developed a partial crosslinking bonding method that reaches 96% bonding yield after three bonding steps. In this method, we found that the bonding yield strongly depends on the difference between the

PEB temperature and the bonding temperature. With PEB at 90 °C and bonding at 100 °C, this method shows similar performance to the CAF technique. However, in the partial crosslinking method, temperature control is critical because at higher PEB temperatures the bonding yield decays rapidly, and at lower temperatures the structure can easily be deformed by the bonding pressure. Conversely, the CAF technique allows bonding of smooth, patterned and hardened layers while still providing enough potential chemical bonds to produce good strength after a thermocompressive bonding step. This decoupling of optimal conditions for bonding and structural stability make the CAF technique better suited to build high-quality multilayer structures.

Acknowledgments

This work was sponsored by the Natural Sciences and Engineering Research Council of Canada NSERC. We would also like to thank Teledyne DALSA Semiconductor, Stephane Martel, and Luc Ouellet for their valuable discussions and support in this work.

References

- [1] Kang K H *et al* 2006 Continuous separation of microparticles by size with direct current-dielectrophoresis *Electrophoresis* **27** 694–702
- [2] Aracil C *et al* 2010 Pneumatic impulsion device for microfluidic systems *Sensors Actuators A* **163** 247–54
- [3] Tsai N C and Sue C Y 2006 SU-8 based continuous-flow RT-PCR bio-chips under high-precision temperature control *Biosens. Bioelectron.* **22** 313–7
- [4] Fluidigm Corporation 2011 <http://www.fluidigm.com/biomark-system.html>
- [5] Micronit Inc 2011 <http://www.micronit.com/research-products/electro-osmotic-flow/>
- [6] Abbott Point of Care Inc. 2010 <http://www.abbottpointofcare.com/>
- [7] Liu C 2007 Recent developments in polymer MEMS *Adv. Mater.* **19** 3783–90
- [8] Weisenberg B and Mooradian D 2002 Hemocompatibility of materials used in microelectromechanical systems : platelet adhesion and morphology *in vitro* *J. Biomed. Mater. Res.* **60** 283–91
- [9] Gutierrez-Rivera L and Cescato L 2008 SU-8 submicrometric sieves recorded by UV interference lithography *J. Micromech. Microeng.* **18** 115003
- [10] Becker H and Gärtner C 2008 Polymer microfabrication technologies for microfluidic systems *Anal. Bioanal. Chem.* **390** 89–111
- [11] del Campo A and Greiner C 2007 SU-8: a photoresist for high-aspect-ratio and 3D submicron lithography *J. Micromech. Microeng.* **17** R81–95
- [12] Miller H *et al* 2004 KMPR photoresist process optimization using factorial experimental design *J. Photopolym. Sci. Technol.* **17** 677–84
- [13] Microchem Corp <http://www.microchem.com/products/kmpr.htm>
- [14] Blanco-Carballo V *et al* 2009 Moisture resistance of SU-8 and KMPR as structural material *Microelectron. Eng.* **86** 765–8
- [15] Salm C *et al* 2008 Reliability aspects of a radiation detector fabricated by post-processing a standard CMOS chip *Microelectron. Reliab.* **48** 1139–43
- [16] Convert L *et al* 2008 Rapid prototyping of integrated microfluidic devices for combined radiation detection and plasma separation *Microsystems and Nanoelectronics Research Conf. (Ottawa, Ontario, 15–18 Oct. 2008)* pp 105–8
- [17] Abgrall P *et al* 2007 SU-8 as a structural material for labs-on-chips and microelectromechanical systems *Electrophoresis* **28** 4539–51
- [18] Malinauskas M P *et al* 2012 Femtosecond visible light induced two-photon photopolymerization for 3D micro/nanostructuring in photoresists and photopolymers *Lithuanian J. Phys.* **50** 201–7
- [19] Yu H *et al* 2006 Fabrication of three-dimensional microstructures based on singled-layered SU-8 for lab-on-chip applications *Sensors Actuators A* **127** 228–34
- [20] Dykes J M *et al* 2007 Creation of embedded structures in SU-8 *Proc. SPIE* **6465** 64650N1–12
- [21] Blanco F *et al* 2004 Novel three-dimensional embedded SU-8 microchannels fabricated using a low temperature full wafer adhesive bonding *J. Micromech. Microeng.* **14** 1047–56
- [22] Tuomikoski S and Franssila S 2005 Free-standing SU-8 microfluidic chip by adhesive bonding and release etching *Sensors Actuators A* **120** 408–15
- [23] Carlier J *et al* 2006 High pressure-resistant SU-8 microchannels for monolithic porous structure integration *J. Micromech. Microeng.* **16** 2211–9
- [24] Metz S *et al* 2004 Polyimide and SU-8 microfluidic devices manufactured by heat-depolymerizable sacrificial material technique *Lab Chip* **4** 114–20
- [25] Martel S and Ouellet L 2010 *European Patent Application* EP2204348 (A2)
- [26] Abgrall P *et al* 2005 A novel fabrication method of flexible and monolithic 3D microfluidic structures using lamination of SU-8 films *J. Micromech. Microeng.* **16** 113–21
- [27] Steigert J *et al* 2008 A versatile and flexible low-temperature full-wafer bonding process of monolithic 3D microfluidic structures in SU-8 *J. Micromech. Microeng.* **18** 095013
- [28] Gadre A *et al* 2004 Fabrication of a fluid encapsulated dermal patch using multilayered SU-8 *Sensors Actuators A* **114** 478–85
- [29] Agirregabiria M *et al* 2005 Fabrication of SU-8 multilayer microstructures based on successive CMOS compatible adhesive bonding and releasing steps *Lab Chip* **5** 545–52
- [30] Patel J N *et al* 2008 PDMS as a sacrificial substrate for SU-8-based biomedical and microfluidic applications *J. Micromech. Microeng.* **18** 095028
- [31] Carcano G *et al* 1993 Spin coating with high viscosity photoresist on square substrates—application in the thin film hybrid microwave integrated circuit field *Microelectron. Int.* **10** 12–20
- [32] Forrest J A *et al* 1997 Interface and chain confinement effects on the glass transition temperature of thin polymer films *Phys. Rev. E* **56** 5705–16